



# Tuning, selecting and switching wavelengths in lasers with chirped and sampled fiber Bragg gratings by high-order mode-locking



Yael Sourani, Alexander Bekker, Boris Levit, Baruch Fischer \*

Andrew & Erna Viterbi Faculty of Electrical Engineering, Technion—Israel Institute of Technology, Haifa 32000, Israel

## ABSTRACT

We study wavelength selectable and switchable lasers with two kinds of fiber Bragg grating (FBG) reflectors, based on high harmonic mode-locking frequency addressing near 10 GHz and 25 GHz. We used fiber lasers and also show results with a cavity extended semiconductor laser. The first implementation of the tunable laser uses a chirped FBG. Different wavelengths define slightly different cavity lengths and an effective dispersion and a wavelength is selected by applying a corresponding mode-locking frequency. We obtained a  $\sim 17$  nm wavelength tuning range at the 1550 nm regime. We also summarize results with a cavity extended semiconductor laser by a chirped fiber grating that gave stable 28 addressable and switchable wavelength channels with a spacing of 100 GHz ( $\approx 0.8$  nm). Here we obtained a tuning range of  $\sim 22.4$  nm at the 1550 nm wavelength regime. The second implementation uses multiple sampled FBGs with different reflecting wavelengths, each determines a different cavity length and therefore a different modulation frequency.

## 1. Introduction

Wavelength controllable components, such as lasers, which can operate at several selectable and switchable wavelengths are important for many applications, especially for dynamic wavelength division multiplexing (WDM) networks in fiber optic communication, fiber sensors and optical testing [1–3].

This work contains three parts that we describe below in systems that are based on ring fiber lasers. The lasers consist of erbium doped fiber (edf) as an amplifier and an active mode-locking with modulation and pulse frequencies up to 25 GHz, compatible with nowadays optical communication requirements. We also study the switching time that is found to be limited by relaxation oscillation that we examined in this paper for the special case of edf which is a three level system. In the literature it is commonly analyzed for four-level systems. We also add at the end results with an extended laser diode (LD) cavity with a chirped fiber grating that gave 28 stable addressable and switchable wavelength channels with a spacing of 100 GHz ( $\approx 0.8$  nm) and a switching time of 5–10 ns.

In the first part we present a broadly tunable ring fiber laser with chirped fiber Bragg gratings (CFBG). Due to dispersion, the axial modes of the laser are unevenly spaced and depend on the wavelength and therefore different wavelengths have different modulation frequencies. There were reports of other works using various gratings and CFBGs with fiber and semiconductor optical amplifiers [4–9]. In this work we reached 25 GHz modulation frequency and a tunable range of  $\sim 17$  nm with a fiber laser that is useful for communication purposes.

In the second part we present a tunable ring fiber laser with sampled FBGs (SFBGs). We reported on the basic method of wavelength switching by mode-locking in fiber and semiconductor lasers in former works [7–11]. In this work we first studied the system with one SFBG and examined the effect of a small modulation tuning. Afterward we worked with two and four gratings with different reflecting wavelengths, each determines a different cavity length and therefore a different modulation frequency. We switched and chose the operating wavelength by changing the modulation frequency.

In the third part we studied a system with two uniform FBGs, and as in the previous part, each grating has a different reflecting wavelength, a different cavity length and a different modulation frequency. Here we examined the wavelength switching properties and limitations. We finally mention another tunable laser system of a laser diode with a CFBG and end with a conclusion.

## 2. Tunable fiber laser using chirped FBG

A schematic description of the laser is shown in Fig. 1. It is a ring cavity with a fiber tail coupled to the laser by an optical circulator containing a CFBG that is  $\sim 6$  mm long and have approximately 20 nm optical bandwidth in the C Band. The CFBG was fabricated in our laboratory by a holographic method and its reflectivity spectrum is shown in Fig. 2(d). The ring cavity included erbium doped fiber and was pumped by a laser diode with a 980 nm wavelength. The laser cavity length was  $l \sim 27$  m and therefore the basic cavity resonance frequency

\* Corresponding author.

E-mail address: [fischer@ee.technion.ac.il](mailto:fischer@ee.technion.ac.il) (B. Fischer).

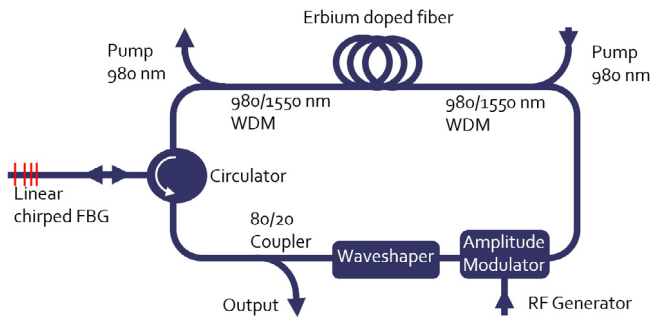


Fig. 1. Schematic of the wavelength switchable fiber laser with CFBG.

was  $\Delta\nu = c/(nl) \approx 7.4$  MHz, where  $c$  is the speed of light and  $n$  is the refractive index of the fiber. When applying a modulation frequency that matches  $\Delta\nu$  or a multiple of it, the axial modes are locked and the laser produces a temporal pulse train at the modulation rate. For reaching the tens GHz regime we operated the laser at high harmonic mode-locking orders,  $\sim 3375$  for 25 GHz and  $\sim 1350$  for 10 GHz, using an amplitude modulator activated by a frequency tunable RF generator. The ring cavity also included a wave-shaper that was used to provide dispersion and loss control.

We can map the mode-locking frequencies to wavelengths in two ways, that can be mapped to each other and considered to be the same. The first one is through the different locations of the Bragg wavelength in the chirped grating that give corresponding mode-locking frequencies due to the different cavity lengths. The other view is by the effective dispersion of the chirped grating that gives a wavelength dependent mode-locking frequency. For the second way, the linear approximation for  $\Delta\nu$  with a dispersion parameter  $D$  near a wavelength  $\lambda_0$  is:  $\Delta\nu(\lambda) \sim c/(nl) - c^2 D (\lambda - \lambda_0) / (n^2 l)$ . Therefore, when the applied modulation frequency equals  $\Delta\nu(\lambda)$  or an harmonics of it, only the axial modes near  $\lambda$  are locked. We also note that in general cases the cavity can include other dispersion sources that causes  $\Delta\nu$  to be a function of the wavelength, but they are usually small in our system unless an intentional dispersion is added as we have below by using a wave-shaper. For harmonic mode-locking of an order  $N$ , where the modulation frequency is  $f_m = N \cdot \Delta\nu(\lambda)$  and  $f_{m0} = N \cdot \Delta\nu(\lambda_0)$ , the generated wavelength varies with  $f_m$ ,

$$\lambda = \lambda_0 - \frac{n^2 l}{N c^2 D} \cdot (f_m - f_{m0}). \quad (1)$$

The dispersion of the CFBG can be evaluated by its length and wavelength range,

$$D_{CFBG} = -\frac{2n_{eff} l_g}{c \Delta\lambda}, \quad (2)$$

where  $n_{eff}$  is the effective refractive index,  $l_g$  is the grating length,  $\Delta\lambda$  is its optical bandwidth and the sign depends on the direction of the chirp. We used an approximated value of  $-3.2$  ps/nm for the calculations done in this work. The dispersion of the fibers and other components in the cavity is approximately 0.4 ps/nm and the dispersion added by the wave-shaper can be varied. The total dispersion is the sum of all these values.

We first set the RF frequency near 10 GHz. By tuning the frequency we obtained mode-locking for various wavelengths, as shown in Fig. 2(a). The widest and most stable mode-locking occurs at the central wavelengths of the grating, where the reflectivity is high and relatively flat as opposed to the edges. For some wavelengths part the modes appear darker due to super-mode noise as shown in Fig. 2(c), the zoom in of Fig. 2(a) near 1553 nm. For achieving a stable temporal pulse train in harmonic mode-locking only one super-mode should oscillate. Simultaneous oscillation of several super-modes is unwanted but happens intermittently.

Fig. 3(a) shows the central wavelength as a function of the RF frequency and its linear fit. The fit has a 4.57 nm/MHz slope which agrees with the calculation according to Eq. (1) that gives 4.82 nm/MHz. The RF range is  $\sim 4$  MHz and the wavelength bandwidth is  $\sim 17.5$  nm, because of the CFBG bandwidth limit. In addition to the optical spectra in Fig. 2(a), the temporal waveforms are shown in Video 1 in the Supplementary Material part for different modulation frequencies at the bottom left side. The green part is enlarged at the bottom right side.

We next use an RF frequency near 25 GHz. We added attenuation by the wave-shaper near 1556 nm to diminish unwanted lasing by increasing its losses. By tuning the frequency we obtained mode-locking for various wavelengths, as shown in Fig. 2(b). Unwanted lasing still appeared at certain wavelengths.

The red dots and the solid line in Fig. 3(b) represent the central wavelength as a function of the RF frequency and its linear fit that has a 1.93 nm/MHz slope which agrees with the calculation according to Eq. (1). The RF range is  $\sim 7.1$  MHz and the wavelength bandwidth is  $\sim 13.6$  nm. In some frequencies, two wavelengths that correspond to the  $N$  and the  $N + 1$  orders of the harmonic mode-locking, are mode locked. In addition to the optical spectra in Fig. 2(b), the temporal waveforms are shown in Video 2 in the Supplementary Material part for different modulation frequencies at the bottom left side. As in the former video, the green part is enlarged at the bottom right side. We next added a dispersion of 1 ps/nm by the wave-shaper, and the blue dots and the dashed line in Fig. 3(b) are the central wavelength and the linear fit as a function of the RF frequency for that case. The RF range is shortened to  $\sim 5.9$  MHz while the wavelength bandwidth is now  $\sim 16.3$  nm.

### 3. Tunable fiber laser using sampled FBGs

A schematic description of the laser is shown in Fig. 4. The cavity is similar to the previous one, but with one or several successive SFBGs in the fiber tail, phase modulator controlled by an RF signal and without a wave-shaper. The SFBGs were also fabricated in our lab. They were all fabricated on one fiber, where each SFBG is composed of four uniform FBG located in close proximity to each other. Each SFBG in the fiber tail has a different central wavelength with reflection lines separated by  $\sim 25$  GHz, each with a width of a few GHz, as shown in Fig. 5. The phase modulator has the same function as the amplitude modulator in the previous case, which is to lock the axial modes when the RF frequency matches  $\Delta\nu$  or a multiple of it, and so producing pulses in the time domain. The laser cavity length was  $l \sim 20$  m and therefore the fundamental frequency was  $\Delta\nu \approx 10$  MHz. In the multiple SFBGs case, each SFBG is placed in a slightly different place along the fiber tail and therefore determines a different resonance frequency. For reaching the 25 GHz regime we operated the laser at high harmonic mode-locking orders ( $\sim 2500$ ).

We first used a fiber tail containing one SFBG near 1560 nm to investigate the effect of slightly different RF frequencies near 25 GHz on the laser spectrum. Two main phenomena were observed: mode-locking and frequency modulation (FM) laser operation.

The FM laser regime occurred when the modulation frequency was detuned from the resonance frequency of the cavity or its harmonics. The spectrum obtained in this case became broader as the RF frequency was closer to the precise mode-locking frequency, and it can be even broader than in the mode-locking regime, but the axial modes are uneven, as expected [12]. The output spectrum in FM laser regime is shown in Fig. 6. In this case, higher RF frequency is closer to the mode-locking frequency and the spectrum is indeed broader.

In the mode-locking regime the spectrum had a Gaussian envelope and the central wavelength was shifted when the RF frequency was varied due to dispersion, as mentioned before. Fig. 7 shows that different modulation frequencies generate mode-locking at different wavelengths. The dispersion in this case is the dispersion of the fibers and all other components in the cavity.

A similar wavelength variation was reached by an equivalent experiment where the modulation frequency remained constant and a linear

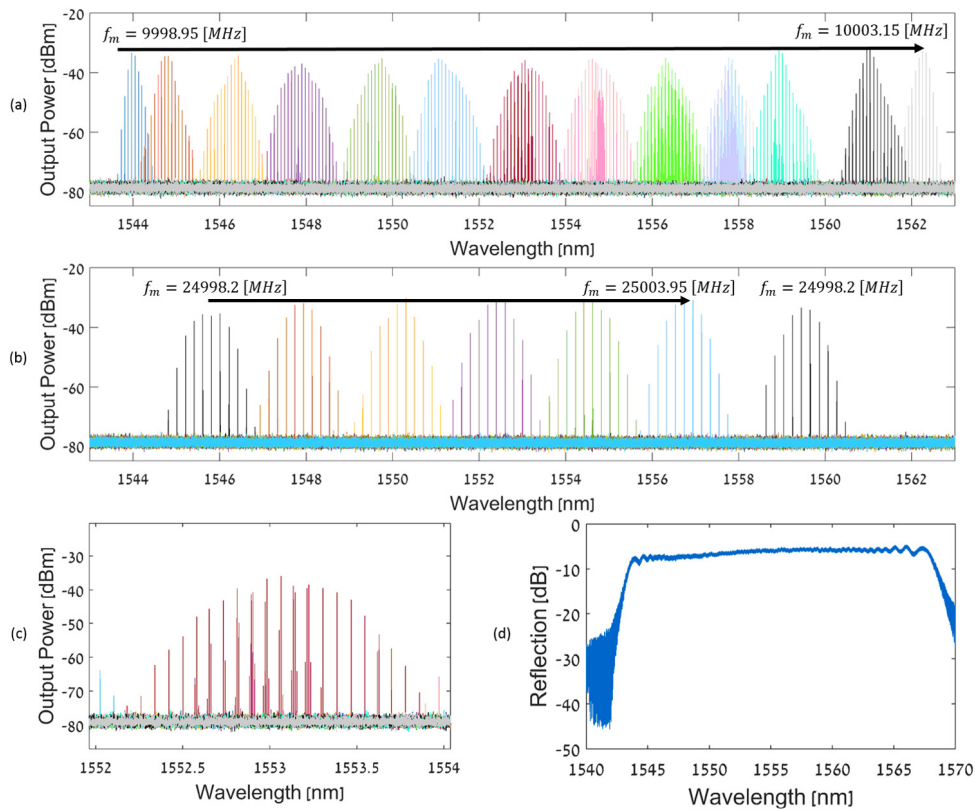


Fig. 2. (a) Output spectra for several modulation frequencies near 10 GHz. (b) Output spectra for several modulation frequencies near 25 GHz. (c) Zoom-in of Fig. 2(a) near 1553 nm. (d) The CFBG reflectivity spectrum.

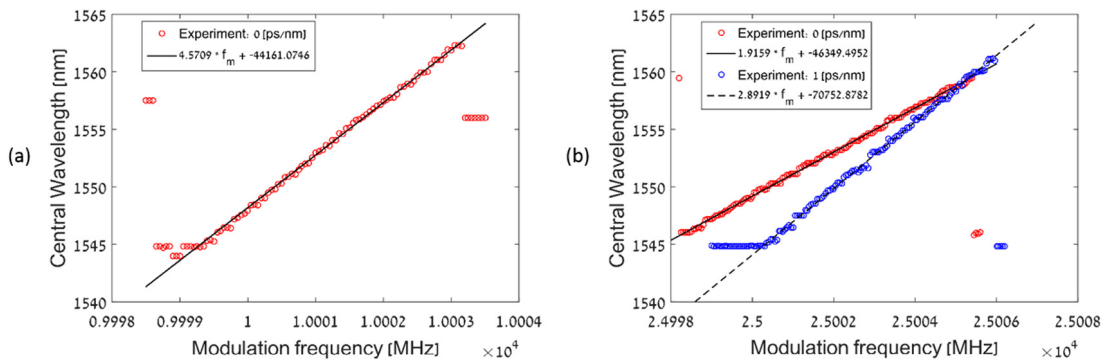


Fig. 3. Central wavelength versus modulation frequency. (a) Experimental results near 10 GHz without added dispersion (red), and their linear fit (black). (b) Experimental results near 25 GHz without added dispersion (red), and their linear fit (black). Experimental results near 25 GHz with 1ps/nm dispersion addition (blue), and their linear fit (dashed black). (For interpretation of the references to color in this figure legend, the reader is referred to the web version of this article.)

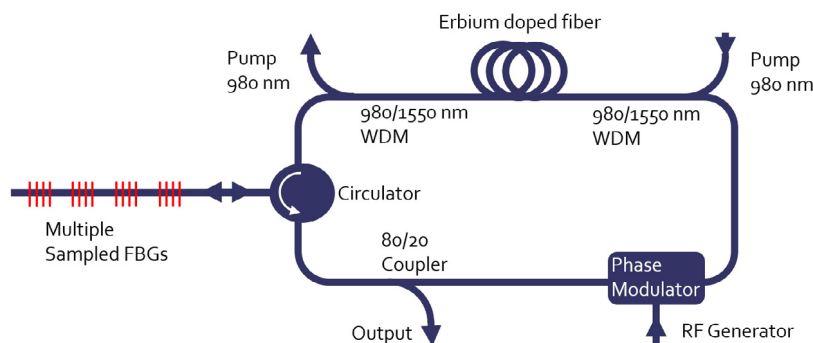


Fig. 4. Schematic of the wavelength switchable fiber laser with multiple SFBGs.

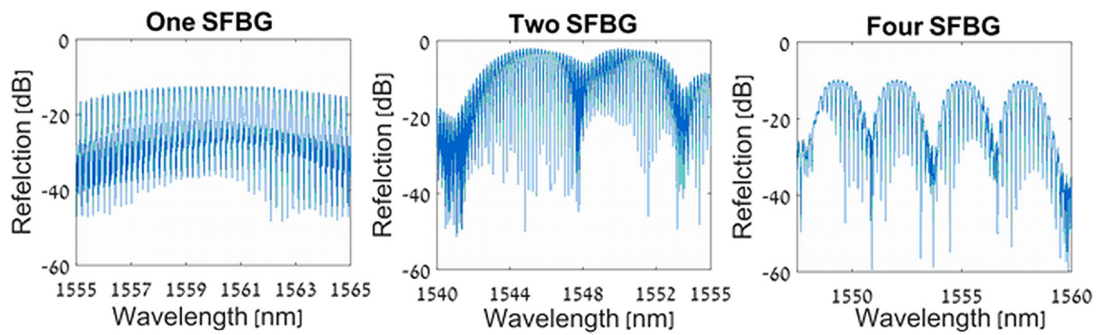


Fig. 5. Reflectivity spectra of one, two and four SFBGs.

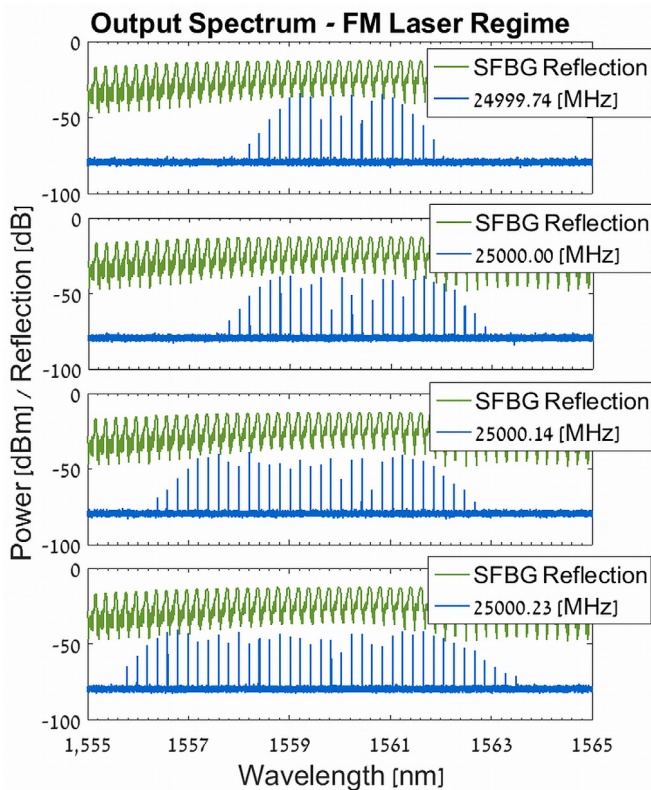


Fig. 6. The output spectrum in the FM laser regime. As the modulation frequency is closer to the cavity resonance the spectrum becomes broader.

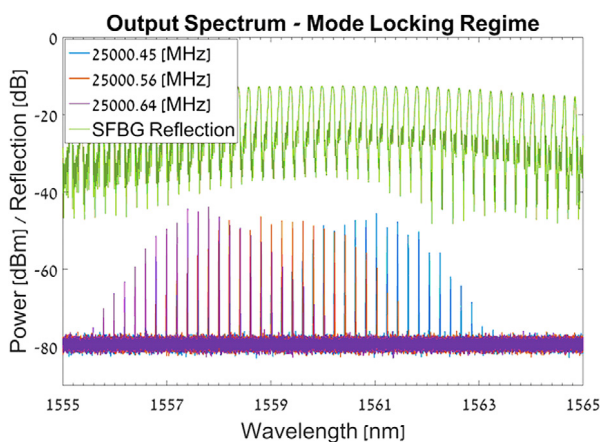


Fig. 7. The output spectrum in the mode-locking regime for the laser with one SFBG. The central wavelength changes when the modulation frequency varies.

phase was applied by a wave shaper inside the ring cavity. The linear phase had a varying slope which affects the difference between two adjacent axial modes of the laser. By this technique we obtained mode-locking and FM lasing exactly as in the previous case, depending on the applied linear slope.

We placed in the fiber laser tail four SFBGs with different wavelengths. Here we could generate mode-locking for each SFBG, choose and switch them by their cavity resonance. The laser was shown to operate at one selectable wavelength, or sometimes in two wavelengths simultaneously, as shown in Fig. 8, depending on the applied RF frequency. Similar results were obtained with two SFBGs, as shown in Fig. 9.

#### 4. Switching properties

An important property of a tunable laser used for communication purposes is the switching time between two wavelengths. For examining this aspect we studied a ring laser similar to the former one but with two successive uniform FBGs connected to the circulator. The FBGs had different reflecting wavelengths in the C-band: one near 1540 nm and the other near 1548 nm. Both had a  $\sim 5$  GHz reflectivity bandwidth. As in the previous case, the modulation frequency of each grating was slightly different so the operating wavelength could be selected by applying the corresponding RF frequency. The laser cavity length was  $l \sim 20$  m, giving a basic cavity resonance frequency of  $\Delta\nu \approx 10$  MHz, and once again we used high order mode-locking. We studied two transitions in the time domain, the first is the switching between one wavelength to the other by changing the RF frequency and the second is the buildup of a certain wavelength by switching-on the RF generator, both transitions were tested while the pump was already active and in a steady state. Fig. 10 shows the switching between two wavelengths, where the power of the second one grows and then stabilizes. In both cases large spikes and oscillations were observed for the built up wavelength. Fig. 11 shows the buildup of 1548 nm with a modulation frequency near 0.5 GHz and a 50 mW pump. Analyzing different modulation frequencies buildup for different pump powers and calculating the oscillations frequencies show a linear relation between the squared oscillations frequency and the pump power, as shown in Fig. 12. Since the modulation frequency is much higher than the oscillations frequency, the laser is assumed to react as CW and the linear relation agrees with a 3 level CW laser analysis of relaxation oscillations. In the calculation of the oscillations frequency we considered a small amplitude fluctuations, and not the spikes, and so it meets the theoretical analysis assumptions of relaxation oscillations. Fig. 12 shows similar results for several modulation frequencies, hence in the GHz mode-locking regime there is no dependence of the oscillations frequency on the modulation frequency, only on the pump power, as explained above. The stabilization of the output could take up to  $\sim 1$  ms. To ensure that the transition between the two frequencies was not caused by the electronics we used a fast RF switch that we designed for this purpose with a switching time of  $\sim 3$  ns between the two RF frequencies, and the same switching behavior was observed.

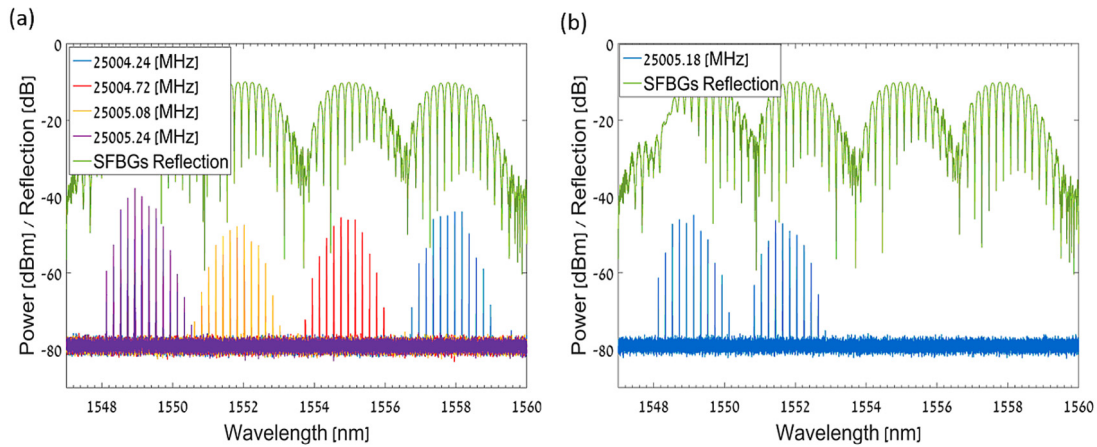


Fig. 8. The output spectrum for the laser with four SFBGs, (a) different modulation frequencies generate mode-locking for a different wavelength, (b) one modulation frequency can generate mode-locking for two wavelengths simultaneously.

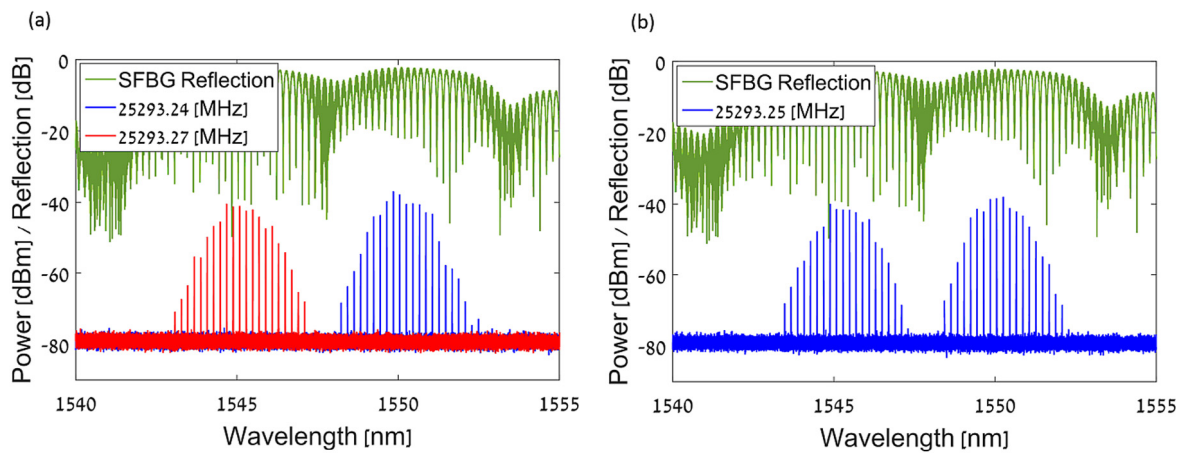


Fig. 9. The output spectrum for the laser with two SFBGs, (a) different modulation frequencies generate mode-locking for different wavelengths, (b) one modulation frequency can generate mode-locking for two wavelengths simultaneously.

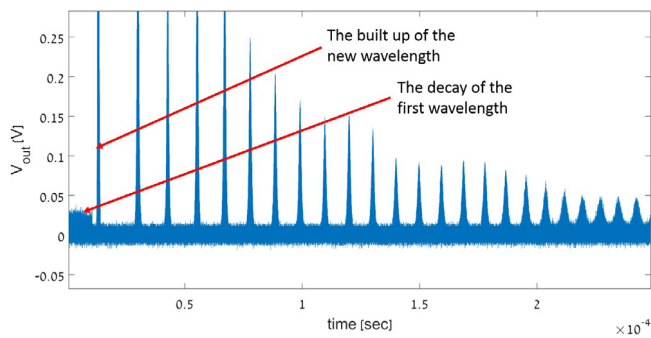


Fig. 10. Switching between two wavelengths.

Similar experiments were performed for the systems with the CFBG and SFBGs, and spikes and oscillations occurred as well, indicating the existence of relaxation oscillations for these system as well.

### 5. Tunable laser based on a laser diode and a CFBG

We add a brief summary of a former work on tunable laser diode (LD) system that was not published yet. The advantage of this system is its small size and length, the possibility to use the basic mode-locking frequency or one of its first harmonics to reach the few or tens GHz

regime, and a fast switching time that can reach the (5–10) ns region without relaxation oscillation. This wavelength tunable LD system is based on mode-locking of a semiconductor LD in an extended cavity that included a chirped fiber grating, similarly to the fiber laser system described above. One of the facets of the LD was anti reflection (AR) coated, to allow a cavity extension, while the back facet was high reflection (HR) coated [7,8], as is schematically shown in Fig. 13.

The laser operates in a mode-locking regime and the emitted wavelength was selected by choosing a modulation frequency that is in resonance with the cavity formed between the HR coated facet and the region of the chirped grating, which reflects the wavelength of interest. Wavelength switching was achieved by slightly changing the RF frequency to that corresponding to a selected wavelength in the chirped grating that matches the mode-locking frequency. The switching time depends on the cavity photon lifetime, and can be reduced to a few ns by a proper cavity design with optimization of the external cavity length and the cavity internal losses. The tunable laser emits pulse trains has a repetition rate that is slightly different for each emitted wavelength, a situation that can cause some limitations, especially when the use of the laser is as an RZ communication source. This can be solved by taking a few pulses, say two, for a bit. It can be also usable as a soliton source. In one implementation [8] the LD amplifier part had a specific length and since the AR coating still had a small residual reflection it still gives a weak Fabry–Perot (FP) grid that can influence, stabilize and fix the overall oscillation. In one case, the longitudinal modes were chosen to have a spacing of  $\sim 100$  GHz ( $\approx 0.8$  nm) that fits the

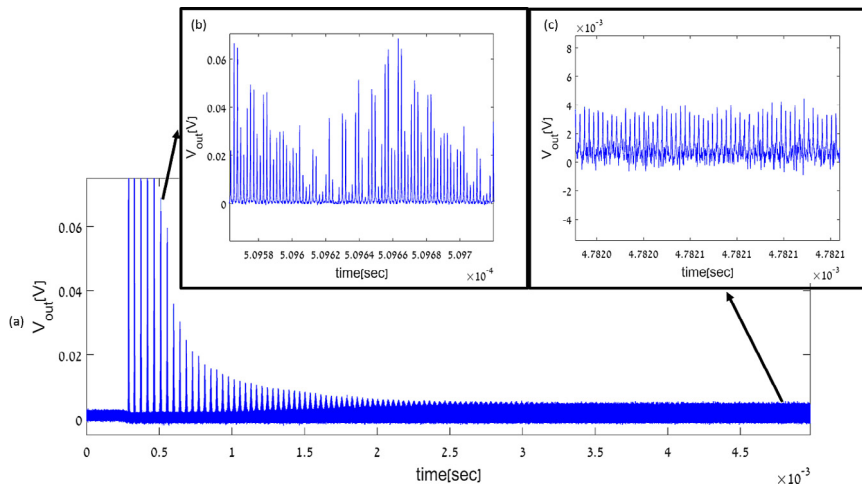


**Fig. 11.** (a) Output voltage stabilization after the RF generator was switched-on near 0.5 GHz for a ring fiber laser connected to a fiber tail containing two FBGs. (b) Zoom-in of a spike. (c) Zoom-in of a steady state.

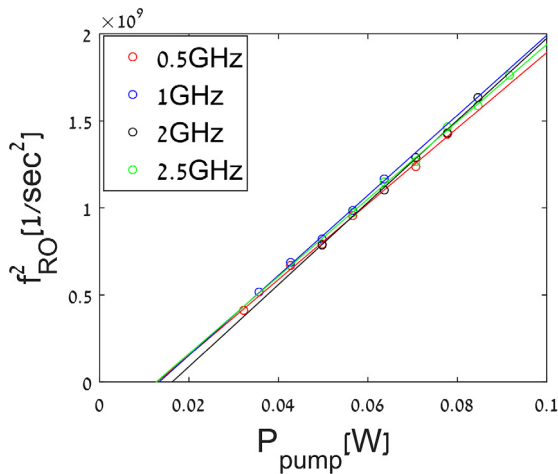


**Fig. 12.** Oscillations frequency squared as a function of the pump power for different modulation frequencies. The circles mark the experimental results and the lines mark the corresponding linear fits.

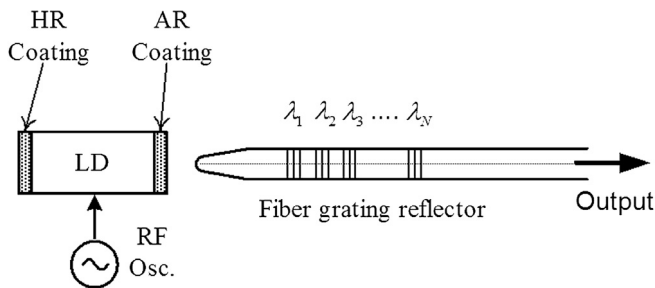


**Fig. 13.** A tunable laser system with a LD gain section extended to a chirped fiber grating.

standard ITU (International Telecommunication Union) channels. The system therefore provides, upon a selective mode-locking frequency, stabilized and fixed wavelength lines by the FP grid matched to specific cavity lengths determined by the chirped grating. The overall length of the extended linear cavity (mostly fiber) was of a few cm long, giving a basic mode-locking frequency of  $\Delta\nu = c/(2nl) \sim (1-5)$  GHz. We even reached with high harmonic mode-locking pulse rates of 40 GHz. To

obtain the different lines we slightly tuned the basic frequency around the basic mode-locking frequency.

To support a large number of wavelengths the total length of the composite grating can become long. This is due to the fact that each wavelength reflector should be isolated in the frequency domain to prevent interference between adjacent reflectors, and therefore its width should be large enough. Short cavity systems would be preferred for a fast wavelength switching time between the different mode-locking frequencies but can complicate the design of the tunable RF synthesizer. In the present experiment we had an overall cavity length (with the continuous chirped grating) of  $\sim 10$  cm, that provided a relatively short switching time on the order of a few (5–10) ns.

Fig. 14 shows the experimental spectral view of the channels as the RF frequency was varied for the tunable LD system with the CFBG. The chirped grating had a relatively flat 40% reflection coefficient in the 1542 to 1564 nm band. The longitudinal modes separation of the LD without the extension was about 98 GHz. We obtained 28 different equally separated wavelengths in the chirped grating reflection window. The figure shows the optical emission spectrum measured by scanning the RF driving frequency and recorded in the maximum hold mode. The laser supported 28 different wavelengths with a tuning range of  $\sim 22.4$  nm. The different RF driving frequencies separation was  $\sim 4$  MHz. Thus, the required RF synthesizer bandwidth (around the central mode-locking frequency) for this laser was about 100 MHz, which is quite small for such a large number of wavelengths. The power variability of the different emitted wavelengths was due to insufficient chirped grating reflectivity flatness.

As explained above, the stability and wavelength selectivity of the laser wavelengths were mostly due to the specifically length design of the LD with its weak FP grid. The outcome was the discrete stable wavelength channels in the measurements shown in Fig. 15. A small deviation of the RF frequency from a specific mode-locking state still gives a wavelength that is on that grid.

We also emphasize that in this system the switching time between wavelength channels was very short, on the order of a few ns, as shown in Fig. 16. It is much shorter than the time we had in the fiber laser, since the wavelength switching time strongly depends on the laser cavity length because changing the wavelength needs a few roundtrip in the cavity before it decays, that is much shorter in the LD system. We also note that we did not observe relaxation oscillation in the LD system case.

## 6. Conclusion

In conclusion, we demonstrated in this work wavelength tunable ring fiber lasers using CFBG or multiple SFBGs and reached the tens

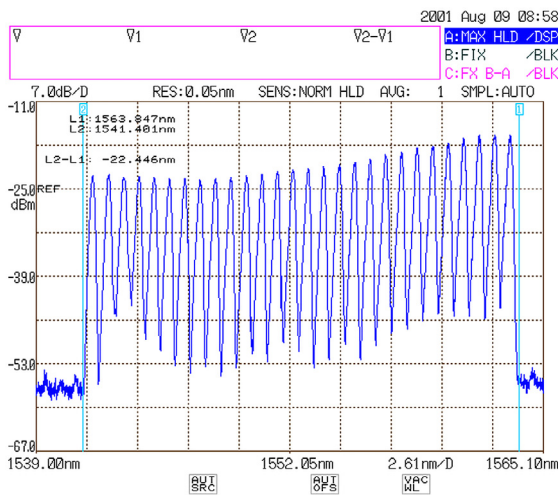


Fig. 14. The spectrum of the tunable laser system of Fig. 13 with a LD gain section extended to a chirped fiber grating. It shows 28 wavelength channels with a ~100 GHz spacing and a ~22.4 nm tuning range.

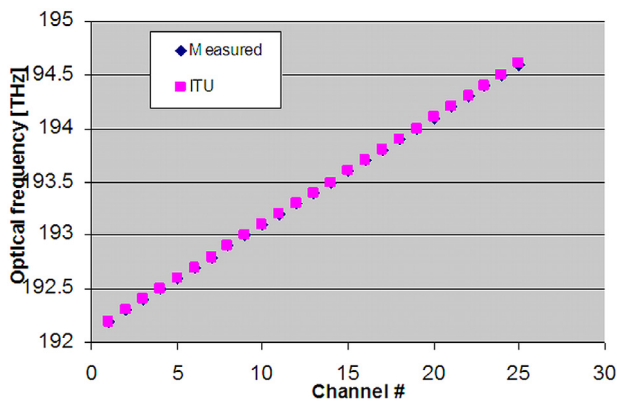


Fig. 15. Measured 25 fixed and stable wavelength channels that fit the ITU grid.

GHz regime by high harmonic mode-locking. For the system with the CFBG we reached ~17.5 nm and ~16.3 nm tuning ranges for 10 GHz and 25 GHz modulation frequencies, respectively. For the systems with the SFBGs we were able to choose between two or four wavelengths, depending on the number of gratings that were used. We encountered two limitation: The first is the super-mode noise which affects the stability of the generated pulses, and the second is relaxation oscillations which limits the transition time between two operating wavelengths. We also described a former system with a semiconductor LD externally coupled to CFBG. It showed a broad tuning range of ~22.4 nm, very short switching times of a few ns, and with a specially designed LD, a very stable grid of wavelength channels. Multi-wavelength lasers are very important for many applications and can be of special uses when the wavelength can be tuned and selected at high speeds.

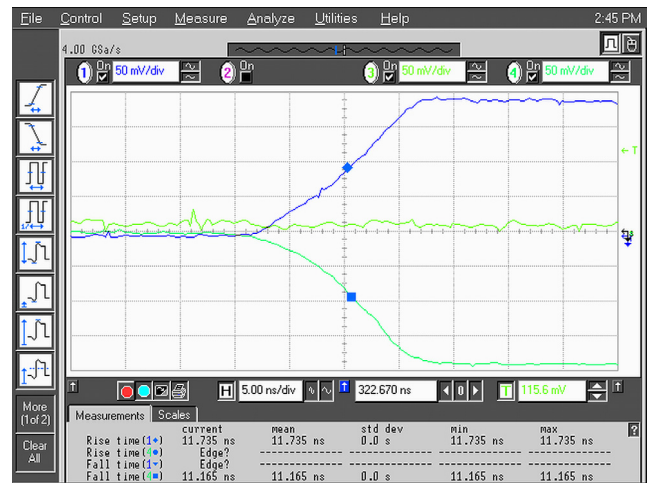


Fig. 16. An example of the power in wavelength switching in the LD system between channels which are 400 GHz apart. The switching time is in the order of 12 ns.

### Acknowledgments

We thank Ron Daisy and Yakir Ovadia for their significant help and role in the measurements done with the tunable LD system.

### Appendix A. Supplementary data

Supplementary material related to this article can be found online at <https://doi.org/10.1016/j.optcom.2018.08.077>.

### References

- [1] A. Bellemare, M. Karasek, M. Rochette, S. L. Rochelle, M. Tetu, Room temperature multifrequency erbium-doped fiber lasers anchored on the ITU frequency grid, *IEEE J. Lightwave Technol.* 18 (2000) 825–831.
- [2] M. Karasek, A. Bellemare, Numerical analysis of multifrequency erbium-doped fibre ring laser employing periodic filter and frequency shifter, *IEE Proc. Optoelectron.* 147 (2000) 115–119.
- [3] K.K. Qureshi, H.Y. Tam, Multiwavelength fiber ring laser using a gain clamped semiconductor optical amplifier, *Opt. Laser Technol.* 44 (2012) 1646–1648.
- [4] B. Burgoyne, A. Villeneuve, Programmable lasers: design and applications, *Proc. SPIE 7580 (758002)* (2010) 758002-15.
- [5] G. Lamouche, S. Vergnole, Y. Kim, B. Burgoyne, A. Villeneuve, Tailoring wavelength sweep for SS-OCT with a programmable picosecond laser, *Proc. SPIE 7889 (78891L)* (2011) 78891L-6.
- [6] Y. Kim, B. Burgoyne, N. Godbout, A. Villeneuve, G. Lamouche, S. Vergnole, Picosecond programmable laser sweeping over 50 mega-wavelengths per second, *Proc. SPIE 7914 (79140Y)* (2011) 79140Y-8.
- [7] B. Fischer, Wavelength-selectable laser system using cavity resonance frequency, especially useful for fiber optic communication and wavelength division multiplexing, US Patent No. US6389047, 2002.
- [8] B. Fischer, Tunable laser with fixed and stable wavelength grid especially useful for WDM in fiber optic communication systems, US Patent No. US7046704, 2006.
- [9] B. Fischer, O. Shapira, B. Levit, A. Bekker, Cavity-resonance-activated wavelength selectable fiber and diode lasers, in: *Conf. on Lasers and Electro-Optics, CLEO'99*, 1999.
- [10] A. Bekker, B. Levit, B. Fischer, Multi-wavelength switchable fiber laser, in: *IEEE 27th convention of Electrical & Electronics Engineers in Israel*, 2012.
- [11] Y. Sourani, A. Bekker, B. Levit, B. Fischer, Wavelength switchable fiber laser with sampled fiber Bragg grating reflectors by mode-locking frequency, in: *2017 Conference on Lasers and Electro-Optics Pacific Rim, CLEO-PR*, 2017.
- [12] A.E. Siegman, *Lasers*, University Science Books, 1986.